Semiconductor Physics, Quantum Electronics & Optoelectronics, 2026. V. 29, No 2. P. 162-171.

Semiconductor physics

Influence of growth-sector structure on electrical characteristics of Schottky and ohmic contacts to boron-doped HPHT diamond

Ya.Ya. Kudryk[1], V.V. Strelchuk[1], D.M. Maziar[1], A.E. Belyaev[1], T.V. Kovalenko[2], A.V. Marchenko[2], V.V. Lysakovskyi[2], S.O. Ivakhnenko[2], M.M. Dub[3,4], P.O. Sai[3,4], W. Knap[3,4], A.S. Nikolenko[1]

[1]*V. Lashkaryov Institute of Semiconductor Physics of NASU, 41 Nauky Avenue, 03028 Kyiv, Ukraine*
[2]*V. Bakul Institute for Superhard Materials of NASU, 2 Avtozavodska Street, 04074 Kyiv, Ukraine*
[3]*CENTERA, CEZAMAT, Warsaw University of Technology, 19 Poleczki Street, 02-822 Warsaw, Poland*
[4]*CENTERA Labs, Institute of High Pressure Physics PAS, 29/37 Sokołowska Street, 01-142 Warsaw, Poland*
[*]*Corresponding author e-mail: nikolenko@isp.kiev.ua*

Abstract. Influence of growth-sector structure on electrical characteristics of Schottky diodes and ohmic contacts fabricated on boron-doped high-pressure high-temperature (HPHT) growth diamond was investigated by correlating electrical measurements with μ-FTIR mapping of uncompensated boron concentration. The studied substrates exhibited pronounced multisectoral inhomogeneity of electrically active boron with systematic variation between the principal growth sectors. The Schottky structures revealed two characteristic transport regimes. In the lower-doped regions, the reverse current was mainly controlled by localized shunting defects, whereas in the higher-doped regions it increased strongly with uncompensated boron concentration and the contacts gradually changed their behavior from rectifying to nearly ohmic one, consistent with increasing contribution of tunneling-assisted transport. The specific contact resistance of the Ti/Pt/Au ohmic contacts decreased with the boron concentration and exhibited clear dependence on growth-sector affiliation. At comparable uncompensated boron concentrations, the contacts formed in the (001) and (113) sectors exhibited lower specific contact resistance than those formed in the (111) sector. The results demonstrate that the growth-sector structure of the boron-doped HPHT diamond influences not only spatial distribution of electrically active boron, but also transport characteristics of metal/diamond contacts therefore representing an important technological factor in fabrication and optimization of diamond-based electronic devices.

Keywords: Schottky barrier, ohmic contact, wide-gap semiconductor, diamond, current-voltage characteristics.

https://doi.org/10.15407/spqeo29.02.162
PACS 73.30.+y, 73.40.Cg, 81.05.ug, 85.30.-z

Manuscript received 14.03.26; revised version received 25.05.26; accepted for publication 10.06.26; published online 23.06.26.

1. Introduction

Diamond is one of the most promising wide-bandgap semiconductors for high-power and high-temperature electronics owing to its high critical electric field strength and carrier mobility, combined with record thermal conductivity [1, 2]. Furthermore, diamond exhibits exceptional radiation resistance, making it ideal for use in space research and other high-radiation environments. At the same time, practical development of diamond electronics remains limited by several materials and technological challenges, including the restricted availability of large-area native substrates, the need for improved crystalline perfection of the device-grade material, and the still insufficient reproducibility of metal/diamond contact technology [1, 2].

Among these limitations, the role of extended structural defects for Schottky and related metal/diamond devices, where electrically active local defects may lead to enhanced reverse leakage, degradation of rectification and premature breakdown [3–6], is especially important. Earlier studies have shown that so-called killer defects can strongly degrade the reverse characteristics of diamond Schottky barrier diodes. In particular, Ohmagari *et al.* demonstrated that local defects in diamond Schottky diodes can be detected in nondestructive ways and are directly related to degradation of the reverse characteristics [3]. Umezawa *et al.* later showed that even under relatively low electric field, a significant fraction of pseudo-vertical diamond Schottky diodes exhibit enhanced leakage current that cannot be explained by conventional transport through the Schottky barrier alone [7].

© V. Lashkaryov Institute of Semiconductor Physics of the NAS of Ukraine, 2026
© Publisher PH "Akademperiodyka" of the NAS of Ukraine, 2026

In that work, the high-leakage state was correlated with the density of deep etch pits revealed after plasma treatment, and the maximum operating voltage decreased with the number of such defect-related pits. These results indicate that the leakage behavior of diamond Schottky diodes is often controlled not only by the ideal barrier properties, but also by discrete crystallographic defects that form localized current paths.

Further studies refined this picture by showing that not only the presence of dislocations themselves, but also the local morphology of the surface in their vicinity, may be critical. Akashi *et al.* demonstrated that threading dislocations affect the characteristics of diamond Schottky barrier diodes [5]. Mikata *et al.* showed that influence of a [001]-directed threading dislocation strongly depends on whether the dislocation region contains pronounced surface irregularities [6]. They found that diodes fabricated on both pyramidal and flat hillocks containing threading dislocations exhibited inferior forward characteristics, but strongly enhanced reverse leakage was observed only for pyramidal hillocks with large surface protrusions, whereas flat hillocks without pronounced surface relief preserved low reverse current. Thus, the electrical effect of a dislocation can be amplified by local near-surface geometry and interface state rather than is defined solely by the dislocation core itself.

The importance of extended defects is not limited to Schottky diodes. Pham *et al.* showed for diamond MOS capacitors that localized electrically active defect spots can serve as conductive leakage paths and distort the capacitance response. These spots were associated with defects containing dislocation bunches [8]. Similarly, Ohmagari *et al.* demonstrated for Schottky diodes on diamond mosaic wafers that coalescence-boundary regions exhibit higher leakage and poorer barrier characteristics, whereas reducing dislocation density leads to much more uniform device performance and breakdown fields above 3 MV cm^{-1} [9]. Thus, the available literature consistently shows that the electrical behavior of metal/diamond structures is highly sensitive to the local defect structure and its effect on the near-surface and interfacial regions.

High-pressure high-temperature (HPHT) growth is one of the most promising methods for obtaining semiconducting single-crystal diamond substrates, since it enables direct incorporation of electrically active boron during bulk crystal growth and allows growth of relatively large crystals [10]. However, single crystals of boron-doped diamond (BDD) typically exhibit a pronounced growth-sector structure. Although a wafer cut from such a crystal remains a single crystal with a common macroscopic orientation, different surface regions originate from different growth faces, most commonly (111), (113), (110), and (001). Because impurity incorporation and defect formation strongly depend on crystallographic growth sector, the resulting wafer is laterally nonuniform with respect to uncompensated boron concentration and related electrical properties [10, 11].

This problem has been already identified by spectroscopic and nanoscale electrical mapping. In our previous studies, correlated Kelvin probe force microscopy, μ-FTIR, and μ-Raman analysis revealed a pronounced growth-sector dependence of uncompensated boron concentration, surface potential, and local strain in multisector boron-doped HPHT diamond [11]. Subsequent investigations of etched HPHT crystals and multisector substrates further demonstrated that sector boundaries and etch-pit regions are accompanied by local electrostructural and morphological heterogeneity [12]. These findings indicate that even in a wafer with a uniform nominal crystallographic orientation, lateral electrical landscape may substantially vary on a scale relevant for contact formation and diode fabrication.

At the same time, the device-level consequences of such growth-sector heterogeneity remain insufficiently clarified. In particular, there are relatively few studies devoted to lateral Schottky structures formed directly on boron-doped HPHT diamond substrates, and even fewer that compare the behavior of Schottky and ohmic contacts within a single multisector crystal. This issue is important because local uncompensated boron concentration is unlikely to be the only controlling parameter. Local defect structure, compensation, and near-surface state of the crystal may also influence barrier height, reverse leakage current, and specific contact resistance. In our recent work on Au/Pt/Ni Schottky diodes on boron-doped HPHT diamond, the current-voltage characteristics (*I–V*) were shown to exhibit hysteresis and voltage-dependent apparent barrier height, which were interpreted in terms of a thin dielectric interfacial gap and deep levels with slow recharging kinetics [13]. That study demonstrated that transport in HPHT-diamond Schottky structures may be controlled not only by bulk doping level, but also by interface-related and trap-related effects.

Against this background, the present work addresses a more specific and technologically important question: how the growth-sector structure of boron-doped HPHT diamond affects the parameters of planar Schottky diodes and ohmic contacts fabricated on the same wafer. Special attention is paid to two interrelated aspects. The first aspect is whether the reverse leakage and yield of low-defect Schottky diodes are defined solely by the local uncompensated boron concentration or are also influenced by sector affiliation. The second aspect is whether the specific contact resistance of ohmic contacts exhibits intrinsic growth-sector dependence at comparable doping levels. Clarification of these issues is important both for physical interpretation of results of transport measurements in multisector HPHT diamond and for optimization of substrate selection and contact technology for diamond-based electronic devices.

2. Experimental details

Single-crystal BDD was grown by the temperature-gradient method under HPHT conditions in a Fe–Al–B–C system at a pressure of 6.5 GPa and temperatures of 1380 to 1420 °C and at a controlled boron content in the growth medium of $2\cdot10^{-4}\ldots10^{-2}$ at.%. The synthesized boron-doped diamond single crystals exhibited cubo-octahedral habit with predominantly developed {111} facets and corresponding growth pyramids (Fig. 1a). Two [001]-oriented

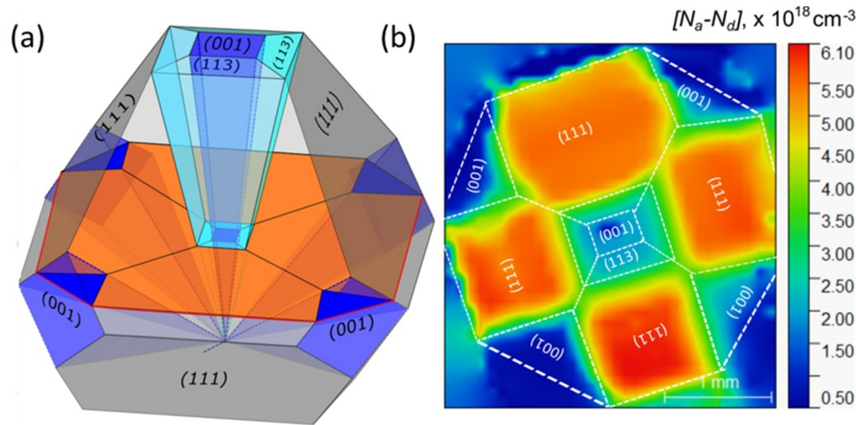

Fig. 1. (a) Schematic representation of a diamond single crystal indicating the crystallographic growth directions and the cutting plane (red line) of the semiconductor wafer. (b) Spatial distribution of uncompensated boron concentration across the wafer surface (sample A), obtained by the μ-FTIR method.

substrates with a thickness of approximately 500 μm, denoted as samples A and B, were mechanically cut from two bulk diamond single crystals with the masses of 106 and 93 mg, respectively, and mechanically polished using a set of cast iron discs and polishing emulsions to the surface RMS roughness of about 0.3 nm for contact formation.

Lateral distribution of the uncompensated boron concentration, $[N_a{-}N_d]$, was determined by μ-FTIR absorption spectroscopy using boron-related absorption bands [14]. Micro-FTIR mapping was performed in transmission mode using a Bruker Hyperion II IR microscope coupled to a Bruker Vertex 70V Fourier-transform spectrometer. The spectra were recorded with 15× Cassegrain objectives in the 650…4000 cm^{-1} range at a spectral resolution of 4 cm^{-1}. Mapping was carried out with a motorized XY stage using a 50 μm step and a 100×100 μm^2 aperture. The uncompensated boron concentration was estimated from the intensities of the boron-related absorption bands at 2800, 2450, and 1290 cm^{-1} according to the procedure described in [14].

The investigated BDD substrates exhibited pronounced multisectoral boron-concentration inhomogeneity, with the boron concentration decreasing in the sequence of the (111), (113), and (001) growth sectors (Fig. 1b). It should be emphasized that the growth-sector structure does not imply variation in crystallographic orientation across the wafer, since the wafer was cut from a single crystal and therefore retained a common macroscopic orientation. The growth-sector structure rather reflects simultaneous growth of several crystallographic faces under the HPHT conditions, each face being characterized by different boron incorporation and defect formation kinetics. As a consequence, different regions of the wafer, referred to as growth sectors, exhibit different uncompensated dopant concentrations. Each sector is denoted by the crystallographic plane corresponding to the growth face that form it, such as (111), (113), or (001).

Frequency histograms of $[N_a{-}N_d]$ and the corresponding in-plane concentration maps were used to identify principal growth sectors and to assign each electrical structure to a given sector (Fig. 2). In both investigated substrates, the highest uncompensated boron concentration was observed in the (111) sector, an intermediate concentration in the (113) sector, and the lowest concentration in the (001) growth sector. The most probable concentrations were $5.5{\cdot}10^{18}$, $1.95{\cdot}10^{18}$, and $0.75{\cdot}10^{18}$ cm^{-3} for the (111), (113), and (001) sectors of the sample A, respectively, and $1.25{\cdot}10^{19}$, $7.8{\cdot}10^{18}$, and $0.8{\cdot}10^{18}$ cm^{-3} for the corresponding sectors of the sample B. These values were used throughout this work as characteristic uncompensated boron concentrations in the respective sectors. The concentration maps also served to identify structures located on the sector boundaries; such structures were excluded from the sector-resolved statistical analysis.

The parameters of the studied substrates A and B are summarized in Table 1. The difference in the dopant concentrations between the sectors increases with the base concentration and may reach an order of magnitude, significantly affecting device performance even when the substrate is used merely as a substrate for CVD diamond layer growth. μ-FTIR–derived histograms of uncompensated dopant concentration distributions across the samples are presented in Fig. 2. The peaks correspond to characteristic concentrations in different growth sectors within the crystal.

To analyze the transport properties and their relation to the defect subsystem, sets of ohmic and Schottky-barrier contacts were fabricated. Before metallization, the samples were subjected to multistep chemical cleaning in order to remove graphite-like surface residues and metallic contamination. The cleaning sequence included

Table 1. Growth-sector-dependent parameters of the investigated boron-doped diamond substrates.

Sample	Orientation	$[N_a-N_d]$, cm^{-3}		
		(111)	(113)	(001)
A	[001]	$5.5{\cdot}10^{18}$	$1.95{\cdot}10^{18}$	$0.75{\cdot}10^{18}$
B	[001]	$1.25{\cdot}10^{19}$	$7.8{\cdot}10^{18}$	$0.8{\cdot}10^{18}$

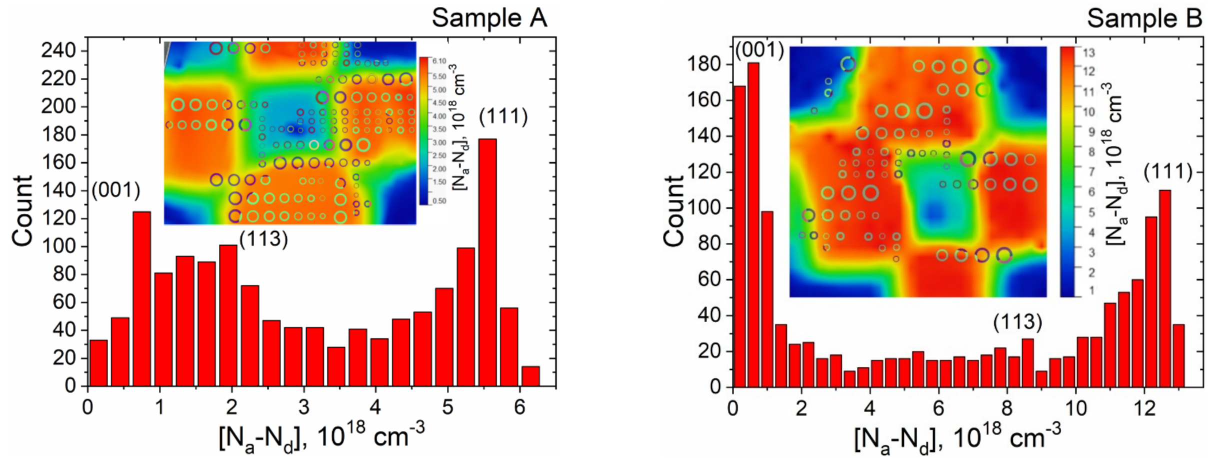

Fig. 2. Frequency distribution of uncompensated dopant concentration across the sample surface obtained by the μ-FTIR method. The inset shows concentration maps of the samples with marked locations of the fabricated diode structures.

treatment in HCl:HNO_3 = 3:1 for 30 min, rinsing in deionized water for 3 min, boiling in H_2SO_4:HNO_3 = 3:2 for 30 min, repeated rinsing in deionized water for 3 min, washing in isopropanol for 5 min, and drying in a nitrogen flow.

The contact structures were formed by optical lithography and metal deposition. A positive photoresist layer (ECI P 3027, MicroChemicals) with a thickness of 2.7 μm was spin-coated at 4000 rpm for 30 s, and the topology was patterned using a 405 nm laser writer. Ohmic contacts were fabricated by deposition of Ti/Pt/Au layers with thicknesses of 38/75/50 nm, followed by lift-off and rapid thermal annealing at 600 °C for 60 s. Schottky barrier contacts were then formed in a second lithography step by deposition of Ni/Pt/Au layers with thicknesses of 75/75/50 nm, followed by rapid thermal annealing at 250 °C for 60 s.

The device layout included arrays of lateral Schottky diodes and transmission-line-model (TLM) test structures (Fig. 3). The topology comprised circular Schottky contacts of different diameters combined with surrounding ohmic pads, as well as linear TLM patterns with interelectrode spacing $L_1 = 10$, $L_2 = 12$, $L_3 = 15$, $L_4 = 20$, $L_5 = 30$, $L_6 = 40$, and $L_7 = 50$ μm, strip width $W = 300$ μm, and contact length $L = 45$ μm.

For the sample A, a total of 150 planar Schottky diodes of various diameters were fabricated, whereas 75 planar Schottky structures were fabricated on the sample B. For analysis of reverse leakage statistics, a subset of equal-area diodes with a barrier-contact radius of 25 μm was selected. Ohmic-contact parameters were evaluated using dedicated TLM structures and were additionally compared with the values inferred from the forward branches of the Schottky-diode *I–V* characteristics. *I–V* characteristics were measured for all the fabricated structures at room temperature. The subsequent statistical analysis was focused on correlating the local uncompensated boron concentration and growth-sector affiliation with the reverse leakage of the Schottky diodes and the specific contact resistance of the ohmic contacts.

3. Results and discussion

The electrical measurements revealed that the growth-sector structure of the investigated BDD substrates affects the transport characteristics at two different levels. First, because the uncompensated boron concentration varies strongly from one growth sector to another, the barrier transparency and the specific contact resistance are intrinsically position-dependent across the substrate surface. Second, superimposed on this smooth sector-related variation, a fraction of the Schottky structures exhibit localized shunting paths that produce anomalously high reverse currents. Thus, the statistical spread of the measured parameters is defined by combined action of sector-dependent doping inhomogeneity and discrete electrically active defects.

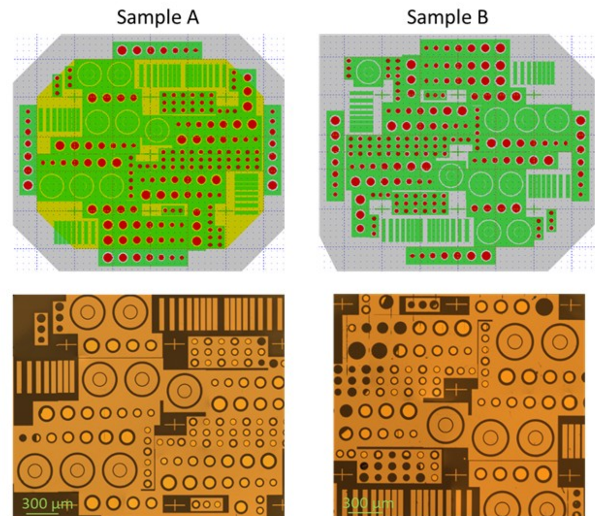

Fig. 3. Layouts of arrays of Schottky diodes, radial and linear TLM structures with ohmic contacts on multisector BDD substrates (top) and fragments of the as-fabricated structures (bottom).

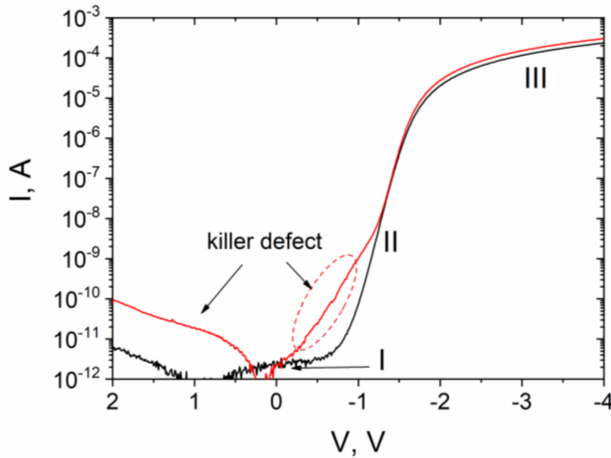

Fig. 4. Current-voltage characteristics of an Au/Pt/Ni/diamond Schottky diode on the sample A: the black curve corresponds to a defect-free diode, while the red curve corresponds to a diode containing a shunting (killer) defect.

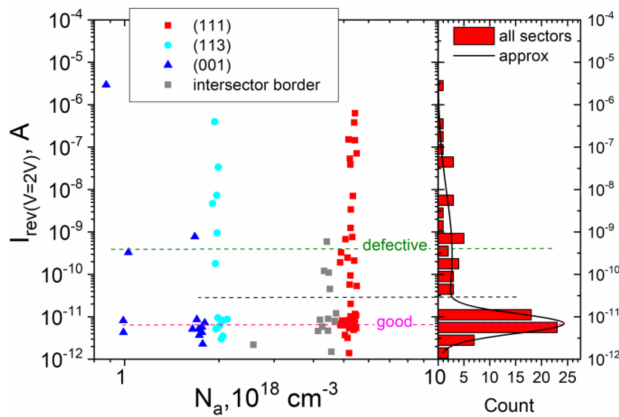

Fig. 5. Dependence of the current at a reverse bias of 2 V on the dopant concentration (sample A). Colors indicate the distribution by growth sectors. On the right – the frequency distribution of current at a 2 V reverse bias is plotted for the entire set of diode structures with a barrier contact radius of 25 μm.

Across the whole set of the fabricated Schottky structures, the *I–V* characteristics exhibited two main types (Fig. 4). The first type corresponds to diodes with well-pronounced rectification and relatively low reverse current. The second type corresponds to structures with enhanced reverse leakage and an additional current contribution at low forward biases, indicating partial shunting of the barrier region. For the defect-free diodes, the forward branch can be conventionally divided into three regions. Region I, close to zero bias, is mainly related to leakage currents of various origins. Region II corresponds to the condition when influence of the series resistance is much lower than the current limitation imposed by the barrier contact and exhibits an exponential behavior. Region III is characterized by a significant effect of the series resistance but also contains a pronounced exponential component, which may be associated with the influence of the ohmic contact. In our previous work on Au/Pt/Ni Schottky diodes, a similar three-region behavior was shown to be sensitive to deep-level recharging and interfacial effects [13]. In the defective diodes, the excess current appears already in Regions I and II and is accompanied by a strongly increased reverse current, which is consistent with the presence of local shunting channels associated with electrically active extended defects of the killer-defect type. Such defects – commonly termed “killer defects” – are typically attributed to dislocations decorated with impurity atoms. When located within the depletion region, they can partially or fully short it, thereby increasing leakage current and reducing breakdown voltage. This interpretation is consistent with earlier studies of defect-controlled transport in diamond, which showed that enhanced leakage in diamond Schottky diodes correlates with defect-related deep etch pits rather than with ideal barrier transport alone [5, 7]. The representative *I–V* characteristics illustrate this contrast between normal rectifying behavior and defect-assisted leakage (Fig. 4).

To analyze the relation between reverse leakage and local electrical activity of substrate, a subset of equal-area diodes with a barrier-contact radius of 25 μm were considered, excluding structures formed at sector boundaries. The dependence of the reverse current at 2 V on uncompensated boron concentration shows that the experimental points are grouped according to the concentration ranges characteristic of the (111), (113), and (001) growth sectors (Fig. 5). However, the most important feature of this distribution is not simply the separation between sectors, but the coexistence of two leakage regimes. One regime corresponds to a large group of diodes with reverse currents clustered in the range of approximately $10^{-12}\ldots3\cdot10^{-11}$ A, which are designated as *“good”*, and an extended tail reaching up to 10^{-6} A, corresponding to *“defective”* diodes (Fig. 5, right). This bimodal behavior indicates that in the lower-doped part of the studied structure set, the reverse current is mainly defined by presence or absence of local shunting defects rather than by a purely monotonic dependence on boron concentration. In other words, the sector-dependent doping level defines the background electrical conditions, but the strongest leakage is caused by discrete local defects.

This interpretation is also supported by the sector-resolved *yield of defect-free diodes* (“quality yield”) summarized in Table 2. This parameter essentially reflects the probability of fabricating a diode without macroscopic defects. The corresponding yields are 60, 54, and 67% for the (111), (113), and (001) sectors, respectively. Although these values are not identical,

Table 2. Quality yield of Schottky diodes by sectors (sample A).

Sector	(111)	(113)	(001)
Total diodes	40	13	15
Defect-free	24	7	10
Yield (%)	60	54	67

they do not follow a simple monotonic trend with uncompensated boron concentration. In particular, the (111) sector, despite having the highest concentration in the substrate A, does not exhibit the lowest yield. Therefore, within the concentration range represented by the less heavily doped substrate, the direct influence of the growth sector on the probability of obtaining a low-leakage Schottky diode is present but comparatively weak. The main factor that distinguishes “good” and “defective” diodes in this regime is occurrence of localized shunting defects rather than the average dopant concentration of a given sector taken alone.

A different behavior is observed when the uncompensated boron concentration approaches and exceeds approximately $9\cdot10^{18}$ cm^{-3}, as in the case of more heavily doped substrate. In this concentration range, the reverse current becomes strongly concentration-dependent, and further doping progressively transforms the contact behavior from clearly rectifying to nearly ohmic one (Figs. 6 and 7). Most structures showed signatures of shunting and/or tunneling currents, predominantly in the (111) sector. This trend is physically expected, since increase in the uncompensated boron concentration reduces the depletion-region width at the metal/diamond interface and enhances tunneling-assisted transport. Within the Padovani–Stratton approach, the forward current in the tunneling regime can be written as follows [15]:

$$I(V) = I_0 \exp(qV/E_0),$$

where $E_0 = E_{00}\coth(qE_{00}/kT)$ and $E_{00} = \frac{\eta}{2}\left[\frac{N_a}{m^*\varepsilon_s}\right]^{1/2}$ is the Padovani–Stratton parameter. Here, m^* is the carrier effective mass and ε_s is the semiconductor permittivity, respectively. The dominant transport regime is defined by the ratio of E_{00} to kT: thermionic emission dominates for $kT/q \gg E_{00}$, thermionic-field emission for $kT/q \approx E_{00}$, and field emission for $kT/q \ll E_{00}$. At room temperature, when kT/q = 0.026 eV, the condition $kT/q \approx E_{00}$ corresponds to $N_a = 8\cdot10^{18}$ cm^{-3}. In the tunneling regime, the saturation current is controlled by the tunneling probability P_t which depends exponentially on the barrier width w:

$$P_t \sim \exp(-B\cdot w).$$

Here, B is a parameter determined by the carrier effective mass and the barrier height. Since the depletion width decreases with the dopant concentration, $w \propto 1/\sqrt{N_a}$, the saturation current is expected to increase approximately as

$$I_s \sim \exp\left(-B/\sqrt{N_a}\right).$$

Therefore, as the dopant concentration increases and the dominant transport mechanism evolves from thermionic emission to thermionic-field emission and finally to field emission, a pronounced increase in the saturation current is expected. Thus, for diodes on the sample B, thermionic emission dominates in the (001) sectors, thermionic-field emission in the (113) sectors, and field emission in the (111) sectors, respectively.

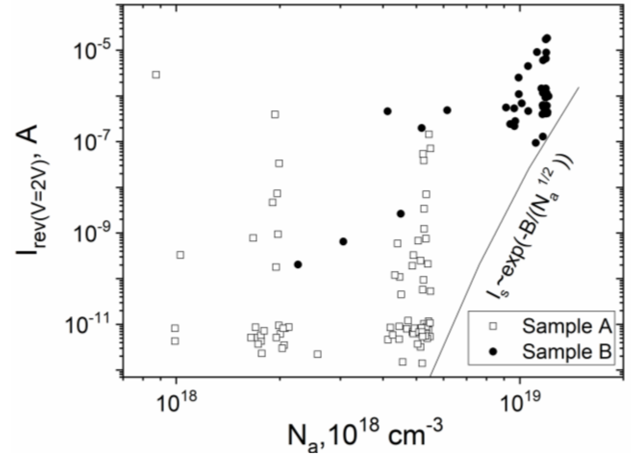

Fig. 6. Dependence of the current at a reverse bias of 2 V on the dopant concentration for both samples A and B.

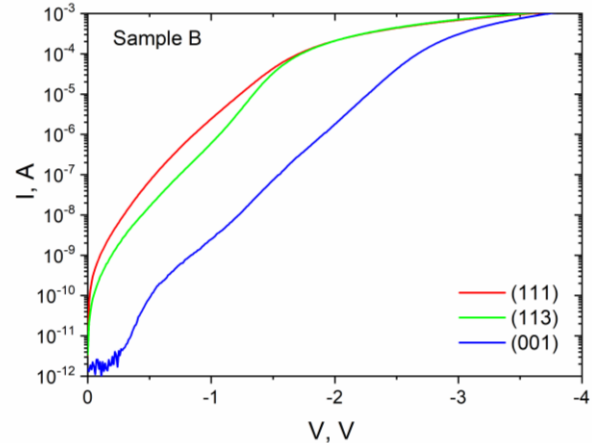

Fig. 7. Current-voltage characteristics of a Au/Pt/Ni/diamond Schottky diode on the sample B for different sectors with varying dopant concentrations.

Accordingly, the (001) regions remain closest to classical Schottky-barrier behavior, the (113) regions correspond to an intermediate regime, and the most heavily doped (111) sectors approach the field-emission limit, where tunneling dominates and rectification is strongly suppressed.

The specific contact resistance is another sensitive parameter reflecting near-surface defects and dopant states. While killer defects contribute negligibly due to their small area fraction, contact resistance can significantly vary with doping and interfacial reactions during rapid thermal annealing (RTA).

The decrease in the specific contact resistance with dopant concentration is consistent with the analysis of Kupka and Anderson [16], who showed that an order-of-magnitude increase in the dopant concentration leads to an approximately order-of-magnitude reduction in the specific contact resistance. In the thermionic-emission regime, the minimum specific contact resistance is given by

$$\rho_{c\,\min} = \frac{k}{qA^*T}\frac{N_c}{N_a},$$

where N_c is the effective density of states in the conduction band. In the same work, the three classical current-transport mechanisms in ohmic contacts, namely thermionic emission, thermionic-field emission, and field emission, were analyzed, and the minimum achievable contact resistance for a given dopant concentration was estimated based on a dominant mechanism. In general, this approach predicts that the minimum specific contact resistance should scale as $\rho_{c\,\min} \sim N_a^{-1}$. However, a stronger dependence can be observed in practice, as can be seen from Figs. 8 and 9, which suggests that additional factors influence the contact behavior and require further investigation.

The behavior of the ohmic contacts is consistent with this overall picture but also reveals an additional sector-related effect. As expected, the specific contact resistance decreases with the uncompensated boron concentration (Figs. 8 and 9), which is consistent with narrowing of the interfacial barrier and transition from thermionic to tunneling-assisted current injection. However, the measured dependence is not described by concentration alone. At comparable uncompensated boron concentration, the contacts fabricated in the (001) and (113) growth sectors generally exhibit lower specific contact resistance than those fabricated in the (111) sector. The same tendency is observed both for the values obtained on dedicated TLM structures and for the estimates derived from the forward branches of the Schottky-diode *I–V* characteristics. This observation indicates an additional growth-sector-related contribution beyond uncompensated boron concentration alone. A plausible origin of this effect is sector-dependent variation of defect structure, compensation, and/or near-surface state of the crystal. Such an interpretation is consistent with our earlier study of similar boron-doped HPHT diamond, in which sectoral boundaries and etched defect regions were shown to exhibit pronounced electrostructural and morphological heterogeneity, including surface-potential steps, local resistivity variations, dislocation-related strain fields, and boron inhomogeneity [12].

This result is important because it indicates that the growth-sector structure affects not only the distribution of electrically active boron, but also the quality of the near-surface region that participates in ohmic-contact formation. In contrast to the case of reverse leakage, where rare killer defects may dominate the current of individual diodes, the specific contact resistance reflects an averaged response over the contact area. Therefore, the observed sector dependence of the contact resistance is unlikely to be explained solely by isolated shunting defects. A more plausible interpretation is that different growth sectors differ not only in the boron concentration, but also in compensation, defect density, and/or the structural state of the near-surface layer formed after polishing and rapid thermal annealing. The present data do not allow unambiguous identification of the microscopic origin of this effect, but they clearly show that equal uncompensated boron concentrations do not guarantee equal ohmic-contact performance in different sectors of the same HPHT crystal.

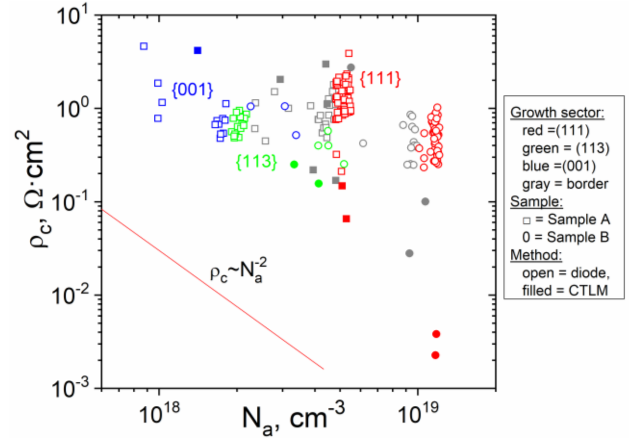

Fig. 8. Specific contact resistance as a function of uncompensated boron concentration for Ti/Pt/Au contacts fabricated on boron-doped HPHT diamond substrates. Colors denote growth sector: (111) – red, (113) – green, (001) – blue, and sector boundary regions – gray. Squares and circles correspond to samples A and B, respectively. Open symbols represent the values estimated from the forward branches of the *I–V* characteristics of the Schottky diodes, whereas filled symbols represent the values obtained from the CTLM measurements.

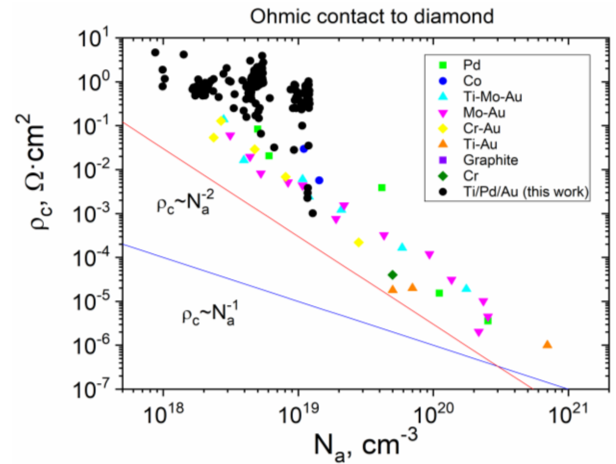

Fig. 9. Dependence of specific contact resistance on the dopant concentration compared with literature data [17].

Overall, the obtained results show that the growth-sector structure must be considered as a technologically important source of lateral electrical nonuniformity in boron-doped HPHT diamond. In the lower-doped regime, the reverse characteristics of Schottky diodes are mainly defined by stochastic occurrence of local shunting defects, while the direct role of sector affiliation in the diode yield is secondary. In the higher-doped regime, the intrinsic effect of the boron concentration on barrier transparency becomes dominant and can drive the metal/diamond contact from rectifying toward nearly ohmic behavior. At the same time, the specific contact resistance of ohmic contacts exhibits a reproducible sector dependence even at comparable doping levels, indicating that growth-

sector-related properties other than the acceptor concentration also influence the electrical characteristics of metal/diamond contacts. These findings are important for both interpretation of transport data and optimization of contact technology for diamond-based electronic devices.

4. Conclusions

The growth-sector structure of boron-doped HPHT diamond was shown to have a pronounced effect on the electrical characteristics of both Schottky diodes and ohmic contacts. The investigated [001]-oriented substrates exhibited strong lateral inhomogeneity of uncompensated boron concentration, decreasing in the sequence of the (111), (113), and (001) growth sectors.

The reverse current of the Schottky structures was controlled by two different factors depending on the doping level. In the lower-doped regime, the leakage current was mainly defined by localized shunting defects, whereas the direct influence of the growth sector on the yield of low-leakage diodes was relatively weak. In the higher-doped regime, the reverse current increased strongly with uncompensated boron concentration, and the most highly doped regions exhibited transition from rectifying to nearly ohmic behavior, consistent with tunneling-assisted transport through a narrowed barrier.

The specific contact resistance of the Ti/Pt/Au ohmic contacts decreased with the boron concentration, as expected, but also showed a clear dependence on growth-sector affiliation. At comparable uncompensated boron concentrations, contacts formed in the (001) and (113) sectors exhibited lower specific contact resistance than those formed in the (111) sector, suggesting an additional contribution related to sector-dependent defect, compensation, or interface-state differences.

These results show that the growth-sector structure of boron-doped HPHT diamond is an important technological factor that must be taken into account in fabrication and optimization of diamond-based electronic devices.

Acknowledgments

This work was supported by the National Research Foundation of Ukraine in the framework of the project No. 2025.07/0197 “Regularities of HPHT-crystallization and physical mechanisms governing the formation of electronic properties of diamond single crystals doped with boron and nitrogen at boundary concentrations”.

This research was also supported by the European Union through the ERC-ADVANCED grant TERAPLASM (No. 101053716). However, the views and opinions expressed here are those of the authors only and do not necessarily reflect those of the European Union or the European Research Council Executive Agency. Neither the European Union nor the granting authority can be held responsible for them. We also acknowledge the support by the “Center for Terahertz Research and Applications (CENTERA2)” project (FENG.02.01-IP.05-T004/23) carried out within the “International Research Agendas” program of the Foundation for Polish Science, co-financed by the European Union under European Funds for a Smart Economy Programme.

Data availability

The data that support the findings of this study will be available on RepOD Repository for Open Data.

References

1. Satoshi K., Hitoshi U., Julien P., Mariko S. (Eds.). *Power Electronics Device Applications of Diamond Semiconductors.* Elsevier, 2018. https://doi.org/10.1016/C2016-0-03999-2.
2. Araujo D., Suzuki M., Lloret F. *et al.* Diamond for electronics: Materials, processing and devices. *Materials* (Basel). 2021. **14**. P. 7081. https://doi.org/10.3390/ma14227081.
3. Ohmagari S., Teraji T., Koide Y. Non-destructive detection of killer defects of diamond Schottky barrier diodes. *J. Appl. Phys*. 2011. **110**. P. 056105. https://doi.org/10.1063/1.3626791.
4. Hanada T., Ohmagari S., Kaneko J.H., Umezawa H. High yield uniformity in pseudo-vertical diamond Schottky barrier diodes fabricated on half-inch single-crystal wafers. *Appl. Phys. Lett*. 2020. **117**. P. 262107. https://doi.org/10.1063/5.0027729.
5. Akashi N., Fujimaki N., Shikata S. Influence of threading dislocations on diamond Schottky barrier diode characteristics. *Diam. Relat. Mater*. 2020. **109**. P. 108024. https://doi.org/10.1016/j.diamond.2020.108024.
6. Mikata N., Takeuchi M., Ohtani N. *et al*. Effect of surface irregularities on diamond Schottky barrier diode with threading dislocations. *Diam. Relat. Mater*. 2022. **127**. P. 109188. https://doi.org/10.1016/j.diamond.2022.109188.
7. Umezawa H., Tatsumi N., Kato Y., Shikata S. Leakage current analysis of diamond Schottky barrier diodes by defect imaging. *Diam. Relat. Mater.* 2013. **40**. P. 56–59. https://doi.org/10.1016/j.diamond.2013.09.011.
8. Pham T.T., Pinero J.C., Marechal A. *et al.* Impact of nonhomoepitaxial defects in depleted diamond MOS capacitors. *IEEE Trans. Electron. Devices*. 2018. **65**. P. 1830–1837. https://doi.org/10.1109/TED.2018.2813084.
9. Ohmagari S., Yamada H., Tsubouchi N. *et al.* Schottky barrier diodes fabricated on diamond mosaic wafers: Dislocation reduction to mitigate the effect of coalescence boundaries. *Appl. Phys. Lett.* 2019. **114**. P. 082104. https://doi.org/10.1063/1.5085364.
10. Lysakovskyi V.V., Novikov N.V., Ivakhnenko S.A. *et al.* Growth of structurally perfect diamond single crystals at high pressures and temperatures. Review. *J. Superhard Mater.* 2018. **40**. P. 315–324. https://doi.org/10.3103/S1063457618050039.
11. Nikolenko A.S., Strelchuk V.V., Lytvyn P.M. *et al.* Correlated Kelvin-probe force microscopy, micro-FTIR and micro-Raman analysis of doping anisotropy in multisectorial boron-doped HPHT diamonds. *Diam. Relat. Mater.* 2022. **124**. P. 108927. https://doi.org/10.1016/j.diamond.2022.108927.
12. Lytvyn P.M., Strelchuk V.V., Nikolenko A.S. *et al.* Electrostructural and morphological features of etch

pits in boron-doped HPHT-diamond single crystals and multisectoral plates. *Diam. Relat. Mater.* 2023. **133**. P. 109752.
https://doi.org/10.1016/j.diamond.2023.109752.
13. Nikolenko A.S., Strelchuk V.V., Kudryk Y.Y. *et al.* Peculiarities of current transport in boron-doped diamond Schottky diodes with hysteresis in current–voltage characteristics. *Diam. Relat. Mater.* 2024. **143**. P. 110897.
https://doi.org/10.1016/j.diamond.2024.110897.
14. Howell D., Collins A.T., Loudin L.C. *et al.* Automated FTIR mapping of boron distribution in diamond. *Diam. Relat. Mater.* 2019. **96**. P. 207–215. https://doi.org/10.1016/j.diamond.2019.02.029.
15. Rhoderick E.H., Williams R.H. *Metal–Semiconductor Contacts*, 2nd ed. Clarendon Press, Oxford, 1988.
16. Kupka R.K., Anderson W.A. Minimal ohmic contact resistance limits to *n*-type semiconductors. *J. Appl. Phys.* 1991. **69**. P. 3623–3632. https://doi.org/10.1063/1.348509.
17. Dub M. Thesis of Doctor of Philosophy: *Investigation of Heat-resistant Ohmic Contacts to Semiconductor Diamond*, V. Lashkaryov Institute of Semiconductor Physics, NAS of Ukraine, 2020.

Authors and CV

Yaroslav Ya. Kudryk, PhD, Senior Researcher at the V. Lashkaryov Institute of Semiconductor Physics, NAS of Ukraine. His scientific interests include solid state physics and transport properties of metal-semiconductor contacts to SiC, GaN, GaP, InP and diamond. E-mail: kudryk@isp.kiev.ua, https://orcid.org/ 0000-0002-5551-2922

Viktor V. Strelchuk, Professor, Doctor of Sciences, Leading Researcher at the Laboratory of Submicron Optical Spectroscopy, V. Lashkaryov Institute of Semiconductor Physics, NAS of Ukraine. Authored over 300 publications, 10 patents, and 6 textbooks. Expertise: physics of semiconductors, Raman and PL spectroscopy of semiconductors and nanostructures.
E-mail: viktor.strelchuk@ccu-semicond.net,
https://orcid.org/0000-0002-6894-1742

Denys M. Maziar, PhD, Researcher at the V. Lashkaryov Institute of Semiconductor Physics, NAS of Ukraine. His research interests include Raman and FTIR spectroscopy of semiconductors, nanostructures and phase-change materials.
E-mail: fmbfiz13.mazyar@kpnu.edu.ua,
https://orcid.org/0000-0002-8906-6107

Alexander E. Belyaev, Professor, Doctor of Sciences, Academician of the NAS of Ukraine. He is the author of more than 220 publications. The area of his scientific activity is transport in quantum multilayer heterostructures and low-dimensional systems and their optical properties as well as application of such structures in UHF devices. E-mail: belyaev@isp.kiev.ua, https://orcid.org/0000-0001-9639-6625

Tetiana V. Kovalenko, PhD, Senior Researcher at the V. Bakul Institute for Superhard Materials, NAS of Ukraine. Her scientific interests cover solution-melt crystallization of diamond at high pressures and temperatures, phase transformations at high pressures, semiconductors, and morphology. Authored over 60 scientific papers and technical patents. https://orcid.org/0000-0003-4878-5161, e-mail: tetiana.v.kovalenko@gmail.com

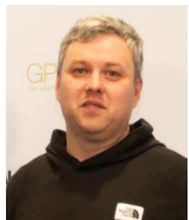

Anton V. Marchenko, PhD student at the V. Bakul Institute for Superhard Materials, NAS of Ukraine, under the supervision of Dr. V.V. Lysakovskyi. His research interests are focused on the synthesis and characterization of superhard materials, high-pressure and high-temperature processes, and diamond crystal growth. E-mail: a.kimarchenko@gmail.com,
https://orcid.org/0009-0003-2305-5872

Valentyn V. Lysakovskyi, Doctor of Technical Sciences, Head of Department at the V. Bakul Institute for Superhard Materials, NAS of Ukraine. His scientific interests cover solution-melt crystallization of diamond at high pressures and temperatures, temperature gradient method, phase transformations at high pressures, boron doped diamond, semiconductors, and morphology. E-mail: lysakovskyi81@gmail.com,
https://orcid.org/0000-0003-4306-9115

Sergii O. Ivakhnenko, Professor, Doctor of Technical Sciences, Corresponding Member of the NAS of Ukraine. His scientific interests cover phase transformations in elements and materials at high pressures and temperatures, nucleation and growth kinetics of diamond single crystals in solution-melt systems at high pressures and temperatures. He is the author of more than 300 scientific papers and technical patents.
E-mail: sioz@ismv13.kiev.ua,
https://orcid.org/0000-0002-4796-3416

Maksym M. Dub, PhD, Assistant Professor Researcher at the Center for Advanced Materials and Technologies (CEZAMAT), Warsaw University of Technology and the Center for Terahertz Technology Research and Applications (CENTERA), Institute of High Pressure Physics, Polish Academy of Sciences. His research interests include semiconductor physics, electrical transport and ohmic contacts to wide-band-gap semiconductors, and terahertz plasmonic devices.
E-mail: maksimdub19f94@gmail.com,
https://orcid.org/0000-0002-6898-4638

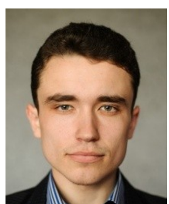

Pavlo O. Sai, PhD, Assistant Professor Researcher at the Center for Advanced Materials and Technologies (CEZAMAT), Warsaw University of Technology and the Center for Terahertz Technology Research and Applications (CENTERA), Institute of High Pressure Physics, Polish Academy of Sciences. His research focuses on semiconductor device physics, terahertz plasmonics, GaN-based high-electron-mobility transistors, and electrical characterization of metal–semiconductor structures. https://orcid.org/0000-0002-6143-9469, e-mail: sajpasha@gmail.com

Wojciech Knap, Professor, Dr. Hab., leader of the CENTERA research program at the Institute of High Pressure Physics, Polish Academy of Sciences, and CEZAMAT, Warsaw University of Technology. His research interests include terahertz physics and electronics, plasmonic phenomena in semiconductor nanostructures, and high-frequency transport in advanced materials. He is a winner of an ERC Advanced Grant and a Foundation for Polish Science Prize for pioneering contributions to terahertz technologies. E-mail: knap.wojciech@gmail.com, https://orcid.org/0000-0003-4537-8712

Andrii S. Nikolenko, PhD, Deputy Head of Department at the V. Lashkaryov Institute of Semiconductor Physics, NAS of Ukraine. His research interests include semiconductor physics, optical spectroscopy of condensed matter (Raman, photoluminescence, and FTIR), optical and electrical properties of wide-bandgap semiconductors, including diamond, as well as semiconductor nanostructures and heterostructures.
https://orcid.org/0000-0001-6775-3451

Authors' contributions

Kudryk Ya.Ya.: methodology, investigation, formal analysis, writing – original draft.
Strelchuk V.V.: funding acquisition, supervision, conceptualization, validation.
Maziar D.M.: investigation, formal analysis.
Belyaev A.E.: conceptualization, validation.
Kovalenko T.V.: investigation, formal analysis.
Marchenko A.V.: investigation, formal analysis.
Lysakovskyi V.V.: investigation, formal analysis.
Ivakhnenko S.O.: conceptualization, resources.
Dub M.M.: methodology, investigation, data curation, visualization.
Sai P.O.: methodology, investigation, data curation, formal analysis.
Knap W.: conceptualization, funding acquisition, supervision.

Вплив секторальної структури росту на електричні характеристики бар'єрів Шотткі та омічних контактів до легованого бором HPHT-алмазу

Я.Я. Кудрик, В.В. Стрельчук, Д.М. Мазяр, О.Є. Бєляєв, Т.В. Коваленко, А.В. Марченко, В.В. Лисаковський, С.О. Івахненко, М.М. Дуб, П.О. Сай, W. Кпар, А.С. Ніколенко

Анотація. Досліджено вплив секторальної структури на електричні характеристики діодів Шотткі та омічних контактів, сформованих на легованому бором HPHT-алмазі, шляхом кореляції електричних вимірювань із мікро-ІЧ картографуванням концентрації нескомпенсованої домішки бору. Досліджені підкладки характеризуються вираженою мультисекторальною неоднорідністю електрично активного бору з систематичними варіаціями між основними секторами росту. У структурах Шотткі виявлено два характерні режими струмопереносу. У слаболегованих областях зворотний струм переважно визначається локалізованими шунтуючими дефектами, тоді як у більш сильнолегованих областях він суттєво зростає зі збільшенням концентрації нескомпенсованого бору, а контакти поступово переходять від випрямляючої поведінки до майже омічної, що узгоджується зі зростанням внеску тунельного струмопереносу. Питомий контактний опір омічних контактів Ti/Pt/Au зменшується зі зростанням концентрації бору, але також виявляє чітку залежність від належності до сектора росту. При близьких значеннях концентрації нескомпенсованого бору контакти, сформовані в секторах (001) та (113), демонструють менший питомий контактний опір порівняно з контактами в секторі (111). Отримані результати свідчать, що секторальна структура росту легованого бором HPHT-алмазу визначає не лише просторовий розподіл електрично активного бору, але й транспортні характеристики контактів метал/алмаз, і тому є важливим технологічним фактором при створенні та оптимізації алмазних електронних приладів.

Ключові слова: бар'єр Шотткі, омічний контакт, широкозонний напівпровідник, алмаз, вольт-амперні характеристики.